

Branching Ratio and Asymmetry for $\Xi^0 \rightarrow \Lambda \gamma$

C. James^(a) and K. Heller

School of Physics and Astronomy, University of Minnesota, Minneapolis, Minnesota 55455

P. Border,^(b) J. Dworkin,^(c) O. E. Overseth, R. Rameika,^(a) and G. Valenti^(d)

Physics Department, University of Michigan, Ann Arbor, Michigan 48109

R. Handler, B. Lundberg,^(a) L. Pondrom, M. Sheaff, and C. Wilkinson^(e)

Physics Department, University of Wisconsin, Madison, Wisconsin 53706

A. Beretvas,^(a) P. Cushman,^(f) T. Devlin, K. B. Luk,^(g) G. B. Thomson, and R. Whitman^(h)

Department of Physics and Astronomy, Rutgers-The State University of New Jersey, Piscataway, New Jersey 08855-0849

(Received 5 September 1989; revised manuscript received 8 January 1990)

We have measured the branching ratio $\Gamma(\Xi^0 \rightarrow \Lambda \gamma)/\Gamma(\Xi^0 \rightarrow \Lambda \pi^0)$ to be $[1.06 \pm 0.12(\text{stat}) \pm 0.11(\text{syst})] \times 10^{-3}$. In 670000 $\Lambda \gamma$ candidates we found $116 \pm 13 \Xi^0 \rightarrow \Lambda \gamma$ decays (background subtracted). These compare with 29510 $\Xi^0 \rightarrow \Lambda \pi^0$ events reconstructed from the $\Lambda \gamma \gamma$ sample. Monte Carlo studies gave the relative acceptances for the two processes. The helicity of the Λ yielded the product of asymmetry parameters $\alpha(\Lambda \rightarrow p \pi^-) \alpha(\Xi^0 \rightarrow \Lambda \gamma) = 0.27 \pm 0.28$, which implies $\alpha(\Xi^0 \rightarrow \Lambda \gamma) = 0.43 \pm 0.44$, where the uncertainty is all statistical.

PACS numbers: 13.40.Hq, 14.20.Jn

Nonleptonic hyperon decays are a means to study the weak interaction in the presence of strong interactions which give rise to important effects such as the $\Delta I = \frac{1}{2}$ rule. Theoretical calculation of weak-to-strong effects yields decay amplitudes and branching ratios for hadron decays, and, for baryons, the decay asymmetry. Although much work has been done to understand baryon decays ($B \rightarrow B' + \text{meson}$), many problems remain.¹ Hyperon weak radiative decays ($B \rightarrow B' + \gamma$) allow the study of simpler systems which retain the essential features of nonleptonic decays.² Until recently, data for testing models of $B \rightarrow B' + \gamma$ have been scarce, with only $\Sigma^+ \rightarrow p \gamma$,³⁻⁵ $\Lambda \rightarrow n \gamma$,⁶ and $\Xi^- \rightarrow \Sigma^- \gamma$ (Ref. 7) to constrain the models. New results on $\Xi^0 \rightarrow \Sigma^0 \gamma$ are now available.⁸ Prior to the present measurement of $\Xi^0 \rightarrow \Lambda \gamma$, only 1 ± 1 event⁹ and an upper limit¹⁰ had been reported.

We report measurements of the branching ratio and asymmetry parameter for $\Xi^0 \rightarrow \Lambda \gamma$ based on 116 ± 13 such events and 29510 $\Xi^0 \rightarrow \Lambda \pi^0$ from an experiment with a neutral-hyperon beam at Fermilab. The main goal was measurement of the transition moment $\mu(\Sigma^0 - \Lambda)$ via Primakoff production from nuclei and subsequent decay $\Sigma^0 \rightarrow \Lambda \gamma$ (Ref. 11) with final-state particles identical to those of the present study. Details are given in Refs. 11-13.

The products of a 400-GeV proton beam interacting with a 4.6-cm lead target (*T1*) were collimated to a neutral beam (~ 3 -mrad production angle, ~ 0.6 -mrad FWHM angular divergence, ~ 1 cm FWHM diam at *C2*) by a 2-mm-diam defining aperture in a 7.3-m, 3.5-T magnet. Figure 1 shows the apparatus used to detect charged particles and γ 's from decays of neutral particles in the beam. A multiwire-proportional-chamber magnetic spectrometer measured the momenta of the

charged particles, and a lead-glass calorimeter detected the γ positions and energies. The trigger required ≥ 1 positive and ≥ 1 negative particle plus a neutral particle in the lead glass depositing ≥ 0.4 GeV in the forward wall (FW) and ≥ 2.5 GeV in the main array (MA). This accepted the following: (a) $\Sigma^0 \rightarrow \Lambda \gamma$, $\Lambda \rightarrow p \pi^-$; (b) $\Xi^0 \rightarrow \Lambda \gamma$, $\Lambda \rightarrow p \pi^-$; and (c) $\Xi^0 \rightarrow \Lambda \pi^0$, $\Lambda \rightarrow p \pi^-$, $\pi^0 \rightarrow 2 \gamma$.

By detecting both hadronic ($\Xi^0 \rightarrow \Lambda \pi^0$) and radiative ($\Xi^0 \rightarrow \Lambda \gamma$) modes simultaneously, effects of the apparatus and analysis were correlated and tend to cancel in the ratio $\Gamma(\Xi^0 \rightarrow \Lambda \gamma)/\Gamma(\Xi^0 \rightarrow \Lambda \pi^0)$. A Monte Carlo (MC) simulation was used to determine the lead-glass response, calculate the apparatus acceptance (with the Ξ^0 momentum spectrum tuned to the data), and study backgrounds. Well constrained (three-constraint) (3-C) $\Xi^0 \rightarrow \Lambda \pi^0$ events with both γ 's identified in the glass agreed well with the MC simulation.^{13,14} For a Ξ^0 produced at *T1* and aimed at the defining beam aperture, the probability of a trigger from a decay with our fiducial volume was 0.16% for $\Xi^0 \rightarrow \Lambda \pi^0$ with both γ 's detected and 0.42% for $\Xi^0 \rightarrow \Lambda \gamma$. For events which satisfied the trigger, the analysis constraints and cuts retained 9.99% of the $\Xi^0 \rightarrow \Lambda \pi^0$ and 14.25% of the $\Xi^0 \rightarrow \Lambda \gamma$. The Λ acceptance was fully correlated for both decays, as were some aspects of the γ identification. The acceptance ratio was $\mathcal{A}(\Xi^0 \rightarrow \Lambda \pi^0)/\mathcal{A}(\Xi^0 \rightarrow \Lambda \gamma) = 0.270 \pm 0.022$. Reasonable variations of cuts and other assumptions in the MC simulation (e.g., Ξ^0 momentum spectrum) were used to determine this uncertainty.

The main backgrounds, $\Xi^0 \rightarrow \Lambda \pi^0$ and $\Sigma^*(1385) \rightarrow \Lambda \pi^0$ (from *T2*) with one missing γ , were studied by (a) dropping the lower-energy γ from two- γ events, (b) examining two- γ events where the two showers coalesce, and (c) MC simulation. Events in the $\Sigma^*(1385)$ mass

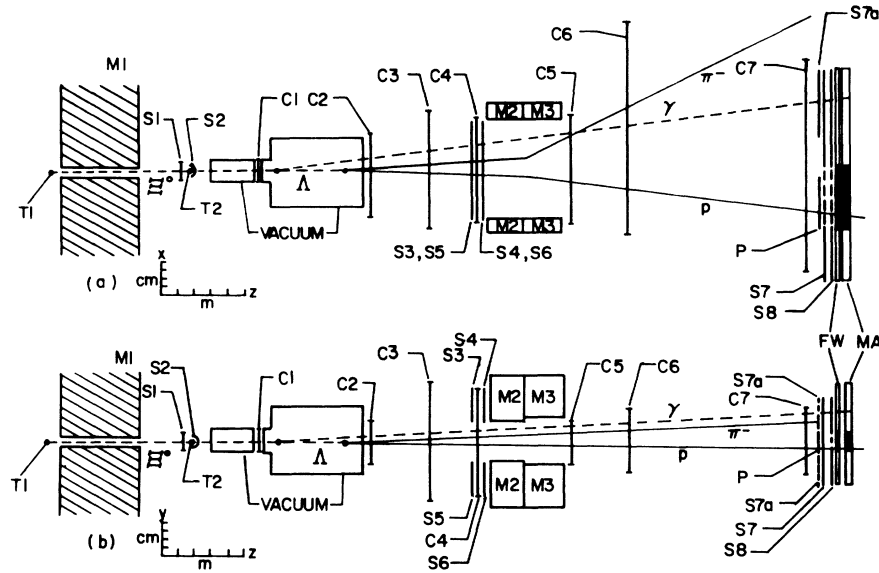


FIG. 1. (a) Plan and (b) elevation views of the detection apparatus. $S1-S7$ and P are scintillation counters. $S1$ and $S2$ surround a target, $T2$, used in the $\mu(\Sigma^0-\Lambda)$ measurement. $C1-C7$ are multiwire proportional chambers. Magnet $M1$ has a 3.5-T field and contains the neutral-beam channel. $M2$ and $M3$ together provide the spectrometer field with a bending power of 1.57 GeV/c. The lead glass consisted of a 3.1- L_{rad} -thick forward wall (FW) and a 12.0- L_{rad} -thick main array (MA). $S3-S6$ constitute a lead-scintillator array to detect γ 's outside the $M2$ aperture.

range with both γ 's detected were reconstructed in the data and show the expected dependence on $T2$ target material. Contributions from other Λ - γ backgrounds, such as beam Λ 's plus accidental γ 's, high-mass Σ^* states produced in $T2$, and $\Xi^0 \rightarrow \Sigma^0 \gamma$, were negligible.

After selecting events with well identified daughter Λ 's

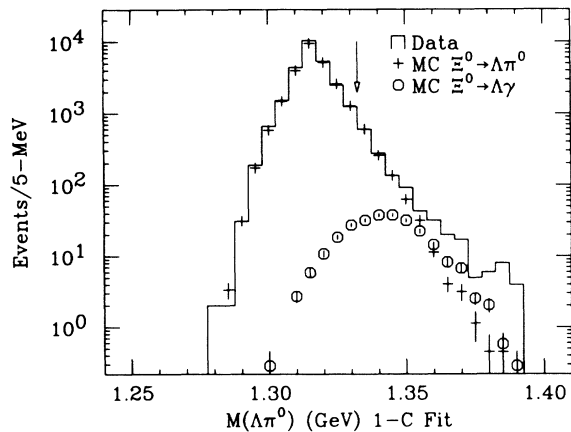


FIG. 2. Histogram of $M(\Lambda\gamma)$ for events with only one γ detected for the data, MC background ($\Xi^0 \rightarrow \Lambda\pi^0$), and MC signal ($\Xi^0 \rightarrow \Lambda\gamma$). A one-constraint fit was performed to determine the *fitted* momentum vectors for the Λ , the detected γ , and for the missing γ . The last was combined with the *measured* momenta to compute $M(\Lambda\pi^0)$ (Ref. 15). Events left of the arrow were cut. The MC background was normalized to fit the data in this plot. The MC signal was normalized to the data after final cuts [see Fig. 3(b)].

not originating in $T1$, a single γ in the calorimeter, Λ transverse momentum $p_{T\Lambda}$ relative to the neutral beam in the range $0.11 \leq p_{T\Lambda} \leq 0.23$ GeV/c, and the invariant mass $M(\Lambda\gamma) \geq 1.24$ GeV, ~ 32000 of the 670000 Λ - γ candidates remained. These were cut to distinguish $\Xi^0 \rightarrow \Lambda\gamma$ from $\Xi^0 \rightarrow \Lambda\pi^0$ with a missing γ . We removed events with either γ energy ≤ 30 GeV or with $0.11 \leq p_{T\Lambda} \leq 0.16$ GeV/c, leaving 1400 events. Next, the mass of each event was reconstructed under a 1-C fit to the hypothesis $\Xi^0 \rightarrow \Lambda\pi^0$ to get the hypothetical missing γ . Its fitted momentum and the measured values of other quantities were used to compute the invariant mass $M(\Lambda\pi^0)$.¹⁵ Figure 2 shows the $M(\Lambda\pi^0)$ distribution for the data and MC-generated samples of $\Xi^0 \rightarrow \Lambda\gamma$ signal events and missing- γ $\Xi^0 \rightarrow \Lambda\pi^0$ background events. We accepted events with $M(\Lambda\pi^0) \geq 3$ standard deviations above $M(\Xi^0)$, leaving 286 events. We removed events with the γ out of the beam-line- P_Λ plane. Finally, to reduce background from $\Sigma^*(1385)$ we cut those with both a computed Ξ^0 decay vertex within 1 m of $T2$ and $p_{T\Lambda} \geq 0.20$ GeV/c.

Figure 3(a) shows a histogram of $M(\Lambda\gamma)$ for the remaining events. It includes a surviving-background MC calculation, which accounts well for events outside the Ξ^0 mass peak. Figure 3(b) shows the background-subtracted distribution along with MC $\Xi^0 \rightarrow \Lambda\gamma$ events subjected to the same cuts and normalized to the signal. The low end of the $M(\Lambda\gamma)$ distribution is truncated by cuts. Both MC simulation and data agree in this as well as the width and centroid.

Between $M(\Lambda\gamma)$ of 1.307 and 1.352 GeV, 160 events

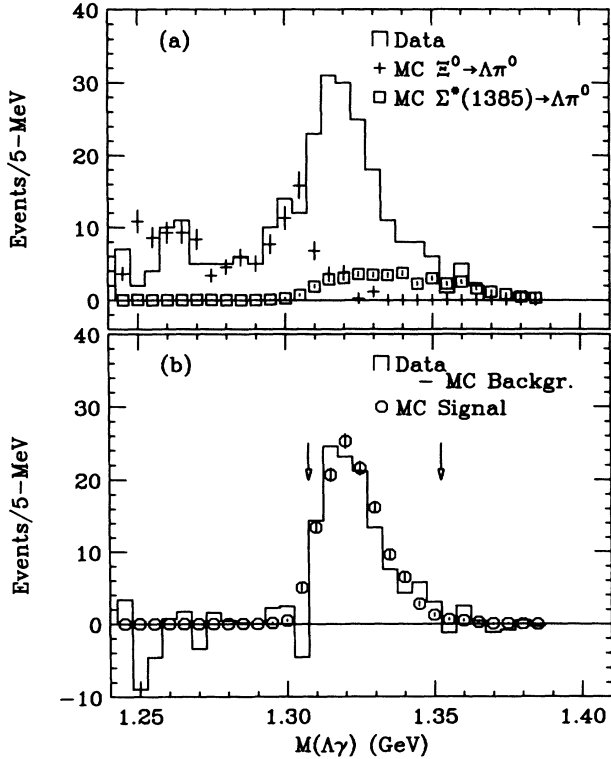


FIG. 3. Histograms of events reconstructed under the hypothesis $\Xi^0 \rightarrow \Lambda\gamma$ after all cuts but the final $M(\Lambda\gamma)$ cut. (a) Data and MC-generated background, i.e., $\Xi^0 \rightarrow \Lambda\pi^0$ and $\Sigma^*(1385)$ with one γ missing. (b) Background-subtracted data and MC-generated $\Xi^0 \rightarrow \Lambda\gamma$ events treated the same way and normalized to the data. Arrows show the cuts used to define the final sample. The MC signal was normalized to fit the data in (b). The MC $\Xi^0 \rightarrow \Lambda\pi^0$ was normalized as in Fig. 2. The MC $\Sigma^*(1385)$ was normalized to two- γ events at target T2.

remained. Estimated backgrounds are 15.6 ± 1.9 $\Xi^0 \rightarrow \Lambda\pi^0$ and 28.5 ± 3.5 $\Sigma^*(1385)$ yielding a signal of 115.9 ± 13.3 $\Xi^0 \rightarrow \Lambda\gamma$ in a data sample containing 29510 $\Xi^0 \rightarrow \Lambda\pi^0$. Corrected for acceptance, this yields

$$\Gamma(\Xi^0 \rightarrow \Lambda\gamma) / \Gamma(\Xi^0 \rightarrow \Lambda\pi^0) = [1.06 \pm 0.12(\text{stat}) \pm 0.11(\text{syst})] \times 10^{-3}.$$

The systematic uncertainty arises mainly from the acceptance.

The product of asymmetry parameters $a(\Lambda)a(\Xi^0)$, where $a(\Lambda) = a(\Lambda \rightarrow p\pi^-)$, was measured through the helicity of the Λ for both processes. For $\Lambda \rightarrow p\pi^-$, the angular distribution of the proton in the Λ rest frame is given by

$$dN/d(\cos\theta_\Lambda) = \frac{1}{2} [1 + a(\Lambda)a(\Xi^0)\cos\theta_\Lambda], \quad (1)$$

where $\cos\theta_\Lambda = \hat{p} \cdot \hat{\Lambda}$, \hat{p} is the proton direction, and $\hat{\Lambda}$ is the Λ direction in the Ξ^0 rest frame ($-\hat{\Lambda}$ is direction of the Ξ^0 in the Λ rest frame). The proton distribution is

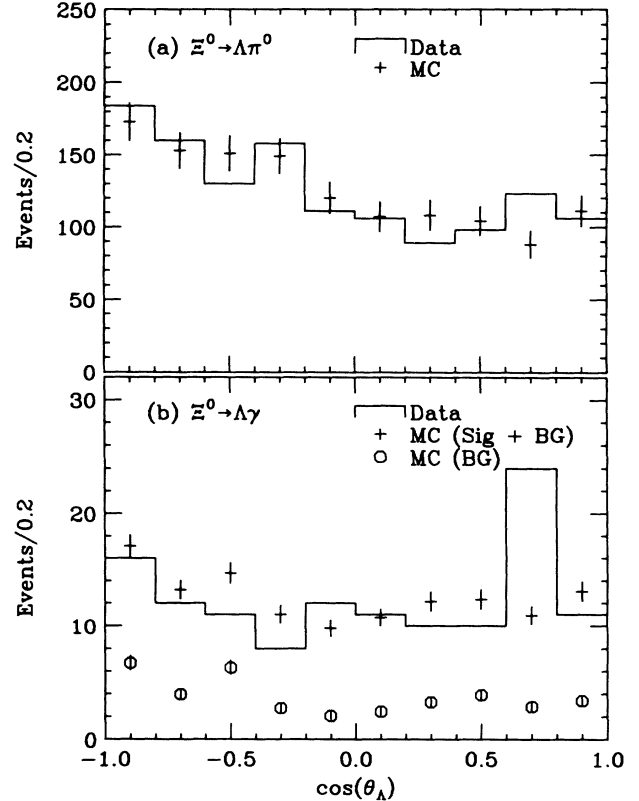


FIG. 4. Histograms of events vs cosine of the helicity angle defined in the text. (a) Fully reconstructed $\Xi^0 \rightarrow \Lambda\pi^0$ data and MC events generated with $a(\Lambda)a(\Xi^0 \rightarrow \Lambda\pi^0) = -0.250$. Hybrid-MC distributions corresponding to each of these agreed well with the plotted distributions and are omitted for clarity. (b) The final $\Xi^0 \rightarrow \Lambda\gamma$ data. MC signal and background events with normalizations and asymmetries described in the text are also plotted.

modified by the acceptance. To correct for this, we used a hybrid MC simulation which took the momentum of the Λ and its position from real events.¹⁶ The hybrid-MC decay angles were chosen from the distribution of Eq. (1) in which the product $a(\Lambda)a(\Xi^0)$ was varied for best fit. A data event was discarded if $< 10\%$ of its hybrid-MC events passed all cuts. This reduced the data events to 125 including background.

Figure 4 shows the $\cos\theta_\Lambda$ distributions. For $\Xi^0 \rightarrow \Lambda\pi^0$, $a(\Lambda)a(\Xi^0 \rightarrow \Lambda\pi^0) = -0.250 \pm 0.017$ with negligible background effects. This agrees with the most precise previous measurement, -0.260 ± 0.004 .¹⁷ For the 125 $\Xi^0 \rightarrow \Lambda\gamma$ candidates, the asymmetry is 0.182 ± 0.195 . The estimated backgrounds are 13.2 ± 1.1 $\Xi^0 \rightarrow \Lambda\pi^0$ (asymmetry = -0.08 ± 0.20) and 24.5 ± 3.0 $\Sigma^*(1385)$ (asymmetry = -0.003 ± 0.082). The background-corrected result is $a(\Lambda)a(\Xi^0 \rightarrow \Lambda\gamma) = 0.27 \pm 0.28$. Division by $a(\Lambda) = 0.642 \pm 0.013$ (Ref. 18) gives $a(\Xi^0 \rightarrow \Lambda\gamma) = 0.43 \pm 0.44$. MC samples of $\Xi^0 \rightarrow \Lambda\gamma$ were generated with different input values of $a(\Lambda)a(\Xi^0 \rightarrow \Lambda\gamma)$, and our

TABLE I. Predictions for $\Xi^0 \rightarrow \Lambda\gamma$ branching fraction and asymmetry.

Ref.	$10^3 \frac{\Gamma(\Xi^0 \rightarrow \Lambda\gamma)}{\Gamma(\Xi^0 \rightarrow \Lambda\pi^0)}$	$a(\Xi^0 \rightarrow \Lambda\gamma)$
20	4.0	
21	7.26	+0.6
22	2.29	-0.41
23	1.4	
24A ^a	1.80	-0.96
24B ^a	1.20	-0.45
25	0.67	-0.29
26	0.72	+0.11
27	2.06	+0.95

^aA and B refer to two solutions in Ref. 24.

analysis recovered those values within 1 standard deviation.

Gaillard¹⁹ first treated $\Gamma(\Xi^0 \rightarrow \Lambda\gamma)$ under various assumptions yielding branching fractions from 0.6×10^{-3} to 31×10^{-3} . Table I lists theoretical calculations made by other authors of the $\Xi^0 \rightarrow \Lambda\gamma$ branching fraction and asymmetries.²⁰⁻²⁷ None agrees with both our branching fraction and asymmetry within 1 standard deviation (statistical and systematic uncertainties combined in quadrature). It is clear that a program of precise measurements of weak radiative decays is necessary to guide the theory.

We thank the staff at Fermilab for making this experiment possible. This work was supported in part by the U.S. Department of Energy and the National Science Foundation.

^(a)Present address: Fermilab, P.O. Box 500, Batavia, IL 60510.

^(b)Present address: School of Physics and Astronomy, University of Minnesota, Minneapolis, MN 55455.

^(c)Present address: Fonar Corporation, 110 Marcus Drive, Melville, NY 11747.

^(d)Present address: CERN, CH-1211, Geneva 23, Switzerland.

^(e)Present address: MP-5, Los Alamos National Laboratory,

P.O. Box 1663, Los Alamos, NM 87545.

^(f)Formerly P. C. Petersen; present address: Physics Department, Yale University, New Haven, CT 06511.

^(g)Present address: Department of Physics, University of California, Berkeley, CA 94720.

^(h)Present address: Philips Medical Systems, 710 Bridgeport Avenue, Shelton, CT 06484.

¹D. Wu. and J. L. Rosner, Phys. Rev. D **26**, 1367 (1986), and references therein.

²M. K. Gaillard, X. Q. Li, and S. Rudaz, Phys. Lett. **158B**, 158 (1985), and references therein.

³S. F. Biagi *et al.*, Z. Phys. C **28**, 495 (1985).

⁴M. Kobayashi *et al.*, Phys. Rev. Lett. **59**, 868 (1987).

⁵N. P. Hessey *et al.*, Z. Phys. C **42**, 175 (1989).

⁶S. F. Biagi *et al.*, Z. Phys. C **30**, 201 (1986).

⁷S. F. Biagi *et al.*, Z. Phys. C **35**, 143 (1985).

⁸S. Teige *et al.*, Phys. Rev. Lett. **63**, 2717 (1989).

⁹N. Yeh *et al.*, Phys. Rev. D **10**, 3545 (1974).

¹⁰J. R. Bensinger *et al.*, Phys. Lett. B **215**, 195 (1988).

¹¹P. C. Petersen *et al.*, Phys. Rev. Lett. **57**, 949 (1986).

¹²P. C. Petersen, Ph.D. thesis, Rutgers University, 1986 (unpublished).

¹³C. James, Ph.D. thesis, University of Minnesota, 1987 (unpublished).

¹⁴Our fit allowed the Ξ^0 decay vertex to vary along the Λ trajectory, constrained by the neutral-beam width.

¹⁵A χ^2 cut on the one-constraint fit is a more conventional alternative. We prefer this equivalent method to show the signal and background in terms of mass resolution.

¹⁶G. Bunce, Nucl. Instrum. Methods **172**, 553 (1980).

¹⁷R. Handler *et al.*, Phys. Rev. D **25**, 639 (1982).

¹⁸Particle Data Group, G. P. Yost *et al.*, Phys. Lett. B **204**, 1 (1988).

¹⁹M. K. Gaillard, Nuovo Cimento **6A**, 559 (1971).

²⁰F. J. Gilman and M. B. Wise, Phys. Rev. D **19**, 976 (1979).

²¹Riazuddin and Fayazuddin, International Centre for Theoretical Physics, Trieste, Report No. IC/79/54, 1979 (unpublished).

²²K. G. Rauh, Z. Phys. C **10**, 81 (1981).

²³P. Eckert and B. Morel, Geneva University Report No. UGVA-DPT 1982/03-340, 1982 (unpublished).

²⁴A. N. Kamal and R. C. Verma, Phys. Rev. D **26**, 190 (1982).

²⁵W. F. Kao and H. J. Schnitzer, Phys. Lett. B **183**, 361 (1987); Phys. Rev. D **37**, 1912 (1988).

²⁶G. Nardulli, Nuovo Cimento **100A**, 485 (1988).

²⁷P. Zenczykowski, Phys. Rev. D **40**, 2290 (1989).